Detecting changes in SAR images based on image fusion using Curvelet Transform

Semeena Latheef [1]

[1] Department of Computer Science Engineering
[1]KMEA Engineering College, Aluva

Abstract— this paper proposes the change detection of SAR images based on image fusion which is done by curvelet transform and classifying changed and unchanged regions by using fuzzy clustering algorithm. The image fusion is a type of data fusion technique is used to generate a difference image by using mean ratio image and log Ratio image. The fused image may provide increased interpretation capabilities and more reliable results since data with different characteristics. Moreover, image fusion can be performed at three different processing levels according to the stage at which the fusion takes: pixel, feature and decision level. Here image fusion done based on curvelet transform which have better shift invariance property end directional selectivity. It is a multi-scale transforms which have the elements identified by scale and location parameter and also the directional parameter. It is an extension of wavelet concept. Curvelet transform represent the edges better than the wavelet transforms. Also a fuzzy local information C-means clustering algorithm is used for classifying the changed and unchanged regions in the fused difference image.

Key words: Image change detection, image fusion, synthetic aperture radar (SAR), FLICM clustering, curvelet transform.

I. INTRODUCTION

Image change detection is a process that analyzes images of the same scene taken at different times in order to identify changes that may have occurred between the acquisition dates [1]. There are large number of applications for this such as remote sensing, medical diagnosis and video surveillance. SAR is Synthetic Aperture Radar image which is one of the major data sources for remote sensing application. It's a high resolution image taken from broad areas of terrain. SAR sensors are independent of atmospheric and sunlight conditions, which make the change detection in SAR images, are very attractive. SAR image reflectivity mainly depends on characteristics of the surface target such as roughness and moisture, as well as on the frequency and incidence angle of the illuminating electromagnetic radiation.

Different kind of applications of SAR images are the following:

1) Land covers monitoring: consist of detecting the seasonal vegetation changes.
2) Land use monitoring: characterization of changes due to human activities like deforestation.
3) Damage mapping: detecting changes caused by natural disasters like earthquake, floods, forest fire etc.

Unsupervised change detection in SAR images can be divided into three steps:

1) image preprocessing
2) Producing difference image between the multi temporal images.
3) Analysis of the difference image.

The tasks of the first step mainly include co-registration, geometric corrections, and noise reduction. In the second step, two co-registered images are compared pixel by pixel to generate the difference image. For the remote sensing images, differencing (subtraction operator) and rationing (ratio operator) are well-known techniques for producing a difference image. In differencing, changes are measured by subtracting the intensity values pixel by pixel between the considered couple of temporal images. In rationing, changes are obtained by applying a pixel-by-pixel ratio operator to the considered couple of temporal images. However, in the case of SAR images, the ratio operator is typically used instead of the subtraction operator since the image differencing technique is not adapted to the statistics of SAR images and non-robust to calibration errors. In addition, because of the multiplicative nature of speckles, the ratio image is usually expressed in a logarithmic or a mean scale. In the third step, changes are usually detected by applying a decision threshold to the histogram of the difference image. Several thresholding methods have been proposed in order to determine the threshold in an unsupervised manner, such as Otsu, the Kittler and Illingworth minimum-error thresholding algorithm (K&I), and the expectation maximization (EM) algorithm.

A. Wavelet Transform

All wavelet transforms are in the forms of time - frequency representation for continuous time signals and related to harmonies analysis. Discrete wavelet transforms normally use discrete - time filter banks and are ca11ed the wavelet & scaling co efficient filter banks consists of finite impulse response (FIR) and infinite impulse response (IIR) filters. Wavelet transforms are subjected to uncertainty principle of Fourier analysis respective sampling theory. Wavelet transforms are classified into three classes continuous, discrete and Multiresolution based.

B. Curvelet Transform

The Curvelet transform has gone through two major revisions. The first generation Curvelet transform used a complex series of steps involving the Ridge let analysis of random transform of an image. The performance was exceeding slow. The second generation Curvelet transforms. Discarded the use of the Ridge let transform, thus reduced the amount of redundancy in the transform and increased the speed considerably.

One of most important characteristic of Curvelet transform is anisotropy which can represent the contour of image more sparsely and provide more information for image processing.

II. MOTIVATION

Here considering the two co-registered intensity SAR images this is acquired over the same geographical area at two different times. Our objective is aiming at producing a difference image that represents the change information between the two times; then, a binary classification is applied to produce a binary image corresponding to the two classes: change and unchanged. The proposed unsupervised distribution-free change detection approach is made up of two main phases:

1) Generate the difference image using the wavelet fusion based on the mean-ratio image and the log-ratio image.
2) Automatic analysis of the fused image by using a fuzzy clustering algorithm.

A. Motivation of Generating Difference Images Using Image Fusion

The ratio difference image is usually expressed in a logarithmic or a mean scale because of the presence of speckle noise. With the log-ratio operator, the multiplicative speckle noise can be transformed in an additive noise component. Furthermore, the range of variation of the ratio image will be compressed and thereby enhances the low-intensity pixels, and in [8], authors proposed a ratio mean detector (RMD), which is also robust to speckle noise. This detector assumes that a change in the scene will appear as a modification of the local mean value of the image. Both methods have yielded effective results for the change detection in SAR imagery but still have some disadvantages: The logarithmic scale is characterized by enhancing the low-intensity pixels while weakening the pixels in the areas of high intensity; therefore, the distribution of two classes (changed and unchanged) could be made more symmetrical. However, the information of changed regions that is obtained by the log-ratio image may not be able to reflect the real changed trends in the maximum extent because of the weakening in the areas of high-intensity pixels. As for the RMD, the background (unchanged regions) of mean-ratio image is quite rough, for the ratio technique may emphasize the differences in the low intensities of the temporal images. In general, the underlying idea of the optimal difference image is that unchanged pixels exhibit small values, whereas changed areas exhibit larger values. That is to say that the optimal difference image should restrain the background (unchanged areas) information and should enhance the information of changed regions in the greatest extent. In order to address this problem, an image fusion technique is introduced to generate the difference image by using complementary information from the mean-ratio image and the log-ratio image in this paper. The information of changed regions reflected by the mean-ratio image is relatively in accordance with the real changed trends in multi-temporal SAR images. On the other hand, the information of background obtained by the log-ratio image is relatively flat on account of the logarithmic transformation. Hence, it can be concluded from the above analysis that the new difference image fused by mean-ratio image and log-ratio image could acquire better information content than the individual difference images (i.e., the mean-ratio image and the log-ratio image).

B. Motivation of Analyzing Difference Image Using Fuzzy Clustering

The purpose to process the difference image is to discriminate changed regions from unchanged regions. The popular method to identify the changed regions, such as the K&I algorithm and the EM algorithm, is usually carried out by applying a thresholding procedure to the histogram of the difference image. It is apparent that this kind of methods requires an accurate estimation of the decision threshold. Moreover, they need to select a proper probability statistical model for distribution of change and unchanged classes in the difference image, which leads to significant restrictions on their application prospect. In this work, a novel fuzzy c-means (FCM) clustering algorithm that is insensitive to the probability statistics model of histogram is proposed to analyze the difference image. Specifically, this method incorporates the information about spatial context to the corresponding objective function for the purpose of reducing the effect of speckle noise.

III. SYSTEM DESIGN

The purpose of this project is to perform image fusion based on curvelet transform instead of wavelet transform. Curvelet transform have better shift invariance property end directional selectivity. It is a multi-scale transforms which have the elements identified by scale and location parameter and also the directional parameter. It is an extension of wavelet concept. Curvelet transform represent the edges better than the wavelet transforms.

The steps of using Curvelet Transform to fuse two images are as follows:

1) Resample and registration of original images, we can correct original images and distortion so that both of them have similar probability distribution. Then Wavelet coefficient of similar component will stay in the same magnitude.
2) Using Wavelet Transform to decompose original images into proper levels. One low-frequency approximate component and three high-frequency detail components will be acquired in each level.
3) Curvelet Transform of individual acquired low frequency approximate component and high frequency detail components from both of images, neighborhood interpolation method is used and the details of grey can't be changed.

IV. SYSTEM IMPLEMENTATION

For the implementation, MatLab version R2008 is used. The standard SAR image from MatLab is considered for performance evaluation. The general steps to be taken for the implementation of the proposed system are as follows:

A. Making log ratio image and mean ratio image

In this module the two source images used for image fusion are obtained from mean ratio operator and log ratio operator respectively which are commonly given by equation (1) and equation (2).

$$X_m = 1 - \min\left(\frac{\mu_1}{\mu_2}, \frac{\mu_2}{\mu_1}\right) \qquad \textbf{(1)}$$

$$X_l = |\log \frac{X_2}{X_1}| = |\log X_2 - \log X_1| \quad \textbf{(2)}$$

Where μ_1 and μ_2 represent local mean values of multi-temporal SAR images X_1 and X_2 respectively.

Here X_m and X_l represent the mean-ratio image and the log-ratio image, respectively.

B. Image fusion using discrete wavelet transform

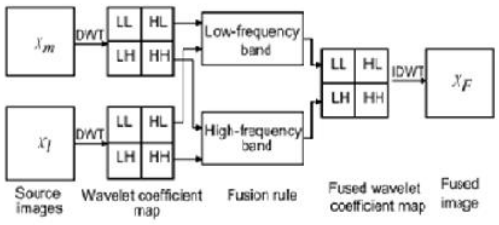

Fig. 2. Process of image fusion based on the DWT

Fig. 1: Process of image fusion based on the DWT

The figure shows the process of image fusion based on Discrete wavelet transform. H and L represent the high-pass and low-pass filters, respectively. In addition, LL represents the approximate portion of the image, and LH, HL, and HH denotes the horizontal, vertical, and diagonal direction portions, respectively. X_F denotes the fused image.

As shown in figure 1, each source image is decomposed into four images of the same size after one level of decomposition. The low-frequency sub band X^{LL1}, which is called the approximation portion, represents the profile features of the source image. Three high-frequency sub bands X^{LH1}, X^{HL1} and X^{HH1} and which correspond to the horizontal, vertical, and diagonal direction portions, show the information about the salient features of the source image such as edges and lines. It can be inferred that the approximate coefficients of the K^{th} decomposition level can be obtained from the approximate and detail coefficients of the $(k+1)^{th}$ level. Furthermore, it is necessary to fuse the wavelet coefficients using different fusion rules for the low-frequency sub band and the high-frequency sub band, respectively, since they represent the different feature information of source images.

Here, two main fusion rules are applied:

1) The rule of selecting the average value of corresponding coefficients for the low-frequency band.
2) The rule of selecting the minimum local area energy coefficient for the high-frequency band.

The fusion rules are described in equation (3) and equation (4).

$$D_{LL}^{F} = \frac{D_{LL}^{m} + D_{LL}^{l}}{2} \quad \textbf{(3)}$$

$$D_e^{F}(i.j) = \begin{Bmatrix} D_e^{m}(i.j), E_\varepsilon^{m}(i,j) < E_\varepsilon^{l}(i,j) \\ D_\varepsilon^{l}(i,j), E_\varepsilon^{m}(i,j) \geq E_\varepsilon^{l}(i,j) \end{Bmatrix}$$

(4)

m and *l* represent the mean-ratio image and the log-ratio image, respectively. *F* denotes the new fused image. D_{LL} stands for low-frequency coefficients. $D_\epsilon(i,j)$ (ϵ = LL,HL,HH) represents three high frequency coefficients at point *(i,j)* in the corresponding sub images.

The local area energy coefficient can be computed using the equation (5).

$$E_\varepsilon(i,j) = \sum_{k\ \varepsilon N_{I,J}} [D_\varepsilon(k)]^2 \quad \textbf{(5)}$$

E_ϵ *(i,j)* represents the local area energy of the wavelet coefficient at point *(i,j)* in the corresponding sub image, and N{i,j} represents the local window centered on *(i,j)*. $D_\epsilon(k)$ denotes the value of the k^{th} wavelet coefficient that is around the local window.

In equation (3) and equation (4), the wavelet coefficients of low frequency and high frequency are fused separately. The low-frequency sub band, which represents the profile features of the source image, can significantly reflect the information of changed regions of two source difference images. Hence, in order to enhance the gradient or edge features of the changed regions, the rule of the average operator is selected to fuse the wavelet coefficients for the low-frequency sub band. On the other hand, for high frequency sub bands, which indicate the information about the salient features of the source image such as edges and lines, the rule of minimum local area energy of wavelet coefficients is selected to suppress the background clutter.

C. Image fusion using curvelet transform

For image fusion curvelet transform is used in proposed work. Here image fusion is done by weighted average method.

The following are the steps for image fusion using curvelet transform.

1) The Curvelet coefficients are weighted.
2) Curvelet coefficients of the multimodal images are computed and fusion is performed by the pixel wise weighted averaging of the constituting images and the approximation coefficients of both input images are added.
3) The resultant sum is multiplied by the random weight 0.2.
4) The weighted average method is tried for various random weights.

D. Analyzing difference image using Fuzzy clustering

The characteristic of FLICM is the use of a fuzzy local similarity measure, which is aimed at guaranteeing noise insensitiveness and image detail preservation. In particular, a novel fuzzy factor G_{ki} is introduced into the object function of FLICM to enhance the clustering performance. This fuzzy factor can be defined mathematically as in equation (6).

$$G_{ki} = \sum_{j \in Ni} \frac{1}{d_{ij}+1} (1-u_{kj}) \wedge m \| x_j - v_j \| \wedge 2$$

(6)

The i^{th} pixel is the center of the local window, the j^{th} pixel represents the neighboring pixels falling into the window around the i^{th} pixel, and d^{ij} is the spatial Euclidean distance between pixels *i* and *j*. v_k represents the prototype of the center of cluster *k*, and u^{kj} represents the fuzzy

membership of the gray value j with respect to the k^{th} cluster.

By using the definition of G_{ki}, the objective function of the FLICM can be defined as in equation (7).

$$Jm = \sum_{i=1}^{N}\sum_{K=1}^{C}\left[u_{ki}{}^{m} \parallel x_i - v_k \parallel^2 + G_{ki}\right] \quad (7)$$

v_k represents the prototype value of the k^{th} cluster and u_{ki} represents the fuzzy membership of the i^{th} pixel with respect to cluster k, N is the number of the data items, and c is the number of clusters. $||x_i\text{-}v_k||^2$ is the Euclidian distance between object x_i and the cluster center v_k.

The calculation of membership partition matrix and the cluster centers is performed as in equation (8) and equation (9).

$$u_{ki} = \frac{1}{\sum_{j=1}^{c}\left(\frac{\parallel x_i - v_k \parallel^2}{\parallel x_i - v_j \parallel^2} + \frac{G_{ki}}{G_{ji}}\right)^{1/(m-1)}} \quad (8)$$

$$v_k = \frac{\sum_{i=1}^{N} u_{ki}{}^{m} x_i}{\sum_{i=1}^{N} u_{ki}{}^{m}} \quad (9)$$

V. ALGORITHMS USED

FLICM algorithm used for clustering is

Step 1: Set the number c of the cluster prototypes, fuzzification Parameter m and the stopping condition ϵ.

Step 2: Initialize randomly the fuzzy partition matrix.

Step 3: Set the loop counter.

Step 4: Compute the cluster prototypes using (9).

Step 5: Calculate the fuzzy partition matrix using (8).

Step 6: max $\{U^{(b)}\text{-}U^{(b+1)}\} < \epsilon$ then stop; otherwise, set b=b+1and go to step 4.

VI. EXPERIMENTAL EVALUATION

The quantitative analysis of change detection results in the proposed method is based on the following parameters.

1) FN - False Negative
2) FP - False Positive
3) PCC - Percentage Correct Classification

First, we calculate the false negatives FN, which is the changed pixel that is undetected.

Second, we calculate the false positives FP, unchanged pixels wrongly classified as changed.

Third, we calculate the percentage correct classification (PCC). It is given by

PCC= (TP +TN) / (TP + FP +TN + FN) (10)

Here, TP is short for true positives, which is the number of pixels that are detected as the changed area in both the reference image and the result.TN is short for true negatives, which is the number of pixels that are detected as the unchanged area in both the reference image and the result [1].

VII. COMPARISON OF PROPOSED WORK

The proposed work is compared with the wavelet transform. From that, we can compare the better efficiency of using the proposed work.

Difference image	FP	FN	PCC
Mean ratio image	12579	31	18.95
Log ratio image	4256	618	68.67
Curvelet fusion	470	761	92.08

Table. 1: Change detection results using curvelet transform

Difference image	FP	FN	PCC
Mean ratio image	12579	31	18.95
Log ratio image	4256	618	68.67
Wavelet fusion	977	735	88.99

Table. 2: Change detection results using wavelet transform

VIII. CONCLUSION

In the proposed system instead of using Discrete Wavelet Transform, Curvelet Transform is used for image fusion. It is a multi-scale transforms which have the elements identified by scale and location parameter and also the directional parameter. Curvelet transform represent the edges better than the wavelet transforms. Compared with the DWT, curvelet transform have a better shift invariance property and directional selectivity. From the experimental evaluation it is found that higher value is obtained for curvelet transform in terms of the parameter percentage correct classification (PCC) when compared to wavelet transform The advantage is that the Curvelet transform will be more efficient and faster than Discrete Wavelet Transform.

REFERENCES

[1] Maoguo Gong, Zhiqiang Zhou, Jingjing Ma, "Change Detection in Synthetic Aperture Radar Images based on Image Fusion and Fuzzy Clustering", IEEE Trans. Image Process., vol. 21, no.4, pp. 294307, April 2012.
[2] R. J. Radke, S. Andra, O. Al-Kofahi, B. Roysam, "Image change detection algorithms: A systematic survey", IEEE Trans. Image Process. Vol. 14, no. 3, pp. 294-307, Mar. 2005.
[3] Bruzzone, D. F. Prieto, "An adaptive semi parametric and context-based approach to unsupervised change detection in multi-temporal remote-sensing images", IEEE Trans. Image Process., vol. 11, no. 4, pp. 452-466, Apr. 2002.
[4] Nielsen, "The regularized iteratively reweighted MAD method for change detection in multi- and hyper spectral data", IEEE Trans. Image Process., vol. 16, no. 2, pp. 463-478, Feb. 2007.
[5] Y. Bazi, L. Bruzzone, F. Melgani, "An unsupervised approach based on the generalized Gaussianmodel to automatic change detection in multi-temporal SAR

images", IEEE Trans. Geosci. Remote Sens., vol. 43, no. 4, pp. 874-887, Apr. 2005.
[6] F. Bovolo, L. Bruzzone, "A detail-preserving scale-driven approach to change detection in multi-temporal SAR images", IEEE Trans. Geosci. Remote Sens., vol. 43, no. 12, pp. 296-2972, Dec. 2005.
[7] F. Bujor, E. Trouv, L. Valet, J. M. Nicolas, J. P. Rudant, "Application of log cumulants to the detection of spatiotemporal discontinuities in multi-temporal SAR images", IEEE Trans. Geosci. Remote Sens., vol. 42, no. 10, pp. 2073-2084, Oct. 2004.
[8] F. Chatelain, J.-Y. Tourneret, J. Inglada, "Change detection in multi- sensor SAR images using bivariate Gamma distributions", IEEE Trans. Image Process., vol. 17, no. 3, pp. 249-258, Mar. 2008.
[9] J. Inglada, G. Mercier, "A new statistical similarity measure for change detection in multi-temporal SAR images and its extension to multi-scale change analysis", IEEE Trans. Geosci. Remote Sens., vol. 45, no. 5, pp. 1432-1445, May 2007.
[10] S. Marchesi, F. Bovolo, L. Bruzzone, "A context-sensitive technique robust to registration noise for change detection in VHR multispectral images", IEEE Trans. Image Process., vol. 19, no. 7, pp. 1877-1889, Jul. 2010.
[11] Robin, L. Moisan, S. Le Hegarat-Mascle, "An a-contrario approach for sub pixel change detection in satellite imagery," IEEE Trans. Pattern Anal. Mach. Intell., vol. 32, no. 11, pp. 1977-1993, Nov. 2010.
[12] M. Bosc, F. Heitz, J. P. Armspach, I. Namer, D. Gounot, L. Rumbach, "Automatic change detection in multimodal serial MRI: Application to multiple sclerosis lesion evolution", Neuroimage, vol. 20, no. 2, pp. 643-656, Oct. 2003.
[13] D. Rey, G. Subsol, H. Delingette, N. Ayache, "Automatic detection and segmentation of evolving processes in 3-D medical images: Application to multiple sclerosis", Med. Image Anal., vol. 6, no. 2, pp. 163-179, Jun. 2002.
[14] D. M. Tsai, S. C. Lai, "Independent component analysis-based background subtraction for indoor surveillance", IEEE Trans. Image Process., vol. 18, no. 1, pp. 158167, Jan. 2009.
[15] S. S. Ho, H. Wechsler, "A martingale framework for detecting changes in data streams by testing exchangeability", IEEE Trans. Pattern Anal. Mach. Intell., vol. 32, no. 12, pp. 2113-2127, Dec. 2010.
[16] A.Singh, "Digital change detection techniques using remotely sensed data", Int. J. Remote Sens., vol. 10, no. 6, pp. 989-1003, 1989.
[17] E. J. M. Rignot, J. J. Van Zyl, "Change detection techniques for ERS-1 SAR data", IEEE Trans. Geosci. Remote Sens., vol. 31, no. 4, pp. 896-906, Jul. 1993.
[18] M. Sezgi, B. Sankur, "A survey over image thresholding techniques and quantitative performance evaluation", J. Electron. Image. vol. 13, no. 1, pp. 146165, Jan. 2004.
[19] S. Krinidis, V. Chatzis, "A robust fuzzy local information C-means clustering algorithm", IEEE Trans. Image Process., vol. 19, no. 5, pp. 1328-1337, May 2010.
[20] E. E. Kuruoglu, J. Zerubia, "Modeling SAR images with a generalization of the Rayleigh distribution", IEEE Trans. Image Process., vol. 13, no. 4, pp. 527-533, Apr. 2004.
[21] G. Piella, "A general framework for multiresolution image fusion: From pixels to regions", Inf. Fusion, vol. 4, no. 4, pp. 259-280, Dec. 2003.
[22] J. C. Bezdek, "Pattern Recognition with Fuzzy Objective Function", New York: Plenum, 1981.
[23] M. Ahmed, S. Yamany, N. Mohamed, A. Farag, T. Moriarty, "A modified fuzzy C-means algorithm for bias _eld estimation and segmentation of MRI data", IEEE Trans. Med. Image., vol. 21, no. 3, pp. 193-199, Mar. 2002.
[24]] W. Cai, S. Chen, D. Zhang, "Fast and robust fuzzy C-means clustering algorithms incorporating local information for image segmentation", Pattern Recognition., vol. 40, no. 3, pp. 825-838, Mar. 2007.
[25] P. L. Rosin, E. Ioannidis, "Evaluation of global image thresholding for change detection", Pattern Recognise. Lett. vol. 24, no. 14, pp. 2345-2356, Oct. 2003.
[26] G. H. Rosenfeld, A. Fitzpatrick-Lins, "A coefficient of agreement as a measure of thematic classification accuracy", Photogram. Eng. Remote Sens., vol. 52, no. 2, pp. 223-227, 1986.

